



The synthesis of melamine-based polyether polyol and its effects on the flame retardancy and physical–mechanical property of rigid polyurethane foam

Yanlin Liu¹, Jiyu He^{1,*}, and Rongjie Yang¹

¹ National Laboratory of Flame Retardant Materials, School of Materials Science and Engineering, Beijing Institute of Technology, 5 South Zhongguancun Street, Haidian District, Beijing 100081, People's Republic of China

Received: 24 October 2016

Accepted: 20 December 2016

Published online:

30 December 2016

© Springer Science+Business Media New York 2016

ABSTRACT

A new type of melamine-based polyether polyol (HMMM–PG) was synthesized based on 1,2-propylene glycol (PG) and hexamethoxy methylene melamine (HMMM). The structure and properties of HMMM–PG were characterized using IR, LC–MS, TG, and shear viscosity analysis, which showed that HMMM–PG had better thermal stability than common polyols as well as shear thinning rheological characteristics. In addition, HMMM–PG was used to prepare polyurethane foams. The compressive strength, thermal conductivity, TG, SEM, LOI, HoC, and XPS were investigated to study the physical–mechanical and fire-retardant properties of the foams. The results showed that the physical–mechanical properties of the foams using HMMM–PG were substantially improved, which was attributed to the higher degree of hydroxyl functionality, which increased the crosslinking density and the number of triazine rings in the structures. Meanwhile, the flame-retardant properties of foams could be significantly improved, which were mainly reflected in the condensed phase. The more stable compounds were retained in the carbon residues during combustion. The continuous and dense char layer was formed. This char layer was effective in preventing heat transfer, and hindered the spread of decomposition products to the flame region.

Introduction

Rigid polyurethane foams (PU/PUF) are widely used in insulation, cushioning, packaging, etc., owing to their low thermal conductivity, superior mechanical properties, and low density [1–4]. However, PU are very combustible and their flame spread is very rapid, which limits their use in stringent fire

situations. For example, as building materials, PU not only need to be able to provide good insulation properties, but also have good flame-retardant properties [5–9]. In addition, flame-retardant standards around the world are now increasing. Therefore, the development of PU with high physical–mechanical properties and excellent flame retardancy is urgently required [10–14].

Address correspondence to E-mail: hejiyu@bit.edu.cn

In general, improvements in the combustion behavior are commonly achieved upon the addition of flame retardants, especially halogen-free flame retardants [15, 16]. Halogenated flame retardants have been abandoned because of environmental and safety problems [17–19]. Melamine is an important flame retardant, since it is rich in nitrogen and has good foaming properties. On the one hand, the dilution of the flame by the sublimated melamine or its decomposition products (NH_3 , CO, and CO_2 , and possibly other volatile products) showed an important effect. On the other hand, the formation of an effective closed char layer, which may involve condensation of melamine to form melam, melem, and related products as well as reactions of the amino and isocyanato groups forming urea derivatives play a key role [20]. For example, it can be used in intumescent flame-retardant systems [21, 22]. The effect of melamine compounds such as melamine polyphosphate and melamine cyanurate on the flame retardant of different polymer materials has been studied, for example, polyamides [23–28], polypropylene [29, 30], ethylene–vinyl acetate copolymer (EVA) [31], epoxy compounds [32], and PU [33, 34]. These melamine compounds are halogen-free, non-corrosive, low smoke, heat and light stabilizers, and inexpensive [33]. However, their shortcomings also need to be considered, i.e., these additive flame retardants are often difficult to process in plastics. In addition, their dispersion in the substrate is poor, so it is difficult to meet the requirements of particle size and distribution. In particular, the addition of a flame retardant will destroy the mechanical properties of the foams.

In principle, an effective way of solving the contradiction between flame retardancy and the physical–mechanical properties is to link the flame retardants to the polymer matrix through chemical covalent linkages [35–37]. Hexamethoxy methylene melamine (HMMM) is a melamine derivative, which has low viscosity and can be converted to polyether polyol. The HMMM-based polyether polyol can be used to substitute parts or all of the polyols and can copolymerize with isocyanate to produce melamine-based foams.

In the present paper, 1,2-propylene glycol (PG) was used to react with HMMM to synthesize the melamine-based polyether polyol. The structural characterization of HMMM–PG and the mechanical properties, thermal stability, and flame retardancy of

the PU using HMMM–PG were systematically studied.

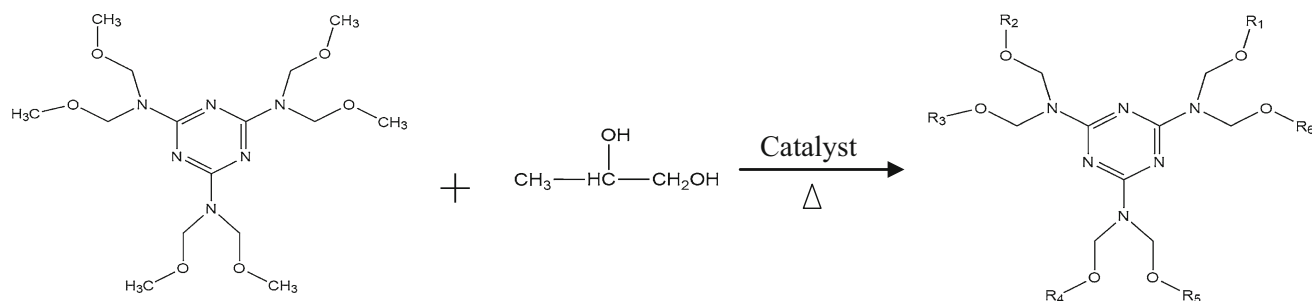
Experimental

Raw materials

- (1) HMMM was provided by Jiangsu Guoli Chemical Technology Co. Ltd. (Jiangsu, China). PG: commercial AR. p-Toluenesulfonic acid, used as catalyst, were purchased from Tianjin Guangfu Fine Chemical Research Institute (Tianjin, China), commercial AR.
- (2) Polyols: 380A, made from poly(propylene oxide) and a sucrose/glycerin base, were purchased from QingdaoLianmei Chemical Co. (Shandong, China). The main properties were as follows: density, 1.15 g cm^{-3} ; typical hydroxyl number, 380A mg KOH/g.
- (3) Silicone glycol copolymer: 8811, used as a surfactant, was purchased from Shanghai Chemical Reagent Co. (Shanghai, China).
- (4) Catalyst: Triethanolamine was used as a crosslinking agent for PU.
- (5) Blowing agent: 1,1-Dichloro-1-fluoroethane (141b) was supplied by Hangzhou Fushite Chemical Industry Co., Zhejiang, China.
- (6) Polymethylene polyphenylene isocyanate (PM-200) was produced by Yantai WanHua, Shandong, China. Polyurethane; NCO content, 31.3 wt%; viscosity $197 \text{ mPa}\cdot\text{s}^{-1}$ ($25 \text{ }^\circ\text{C}$).

Synthesis of HMMM–PG

HMMM (39.02 g, 0.1 mol) and PG (45.62 g, 0.6 mol) were added to a 250-mL three-neck flask with distillation apparatus under a nitrogen atmosphere. p-toluenesulfonic acid (0.77 g, 0.0045 mol) as a catalyst was added under intense stirring. The flask was kept at $160 \text{ }^\circ\text{C}$ in an oil bath for 8 h while being constantly stirred, and the methanol generated was removed by distillation. After the reaction was complete, the heating was stopped and the reaction temperature was cooled to $70 \text{ }^\circ\text{C}$. Then, distillation under reduced pressure to remove the remaining methanol was performed. Finally, the product was obtained in 91.2% yield (59.68 g). Scheme 1 shows the



Scheme 1 The synthesis of HMMM–PG.

Table 1 The formulations of each sample

Component	Samples		
	PUF:380A	PUF:380A/50%HMMM–PG	PUF:HMMM–PG
380A (g)	100	50	0
HMMM–PG (g)	0	42.5	85
8811 (g)	3	3	3
triethanolamine (g)	1.5	1.5	1.5
141b (g)	35	35	35
PM-200 (g)	100	100	100

synthesis of HMMM–PG, where, R_1 – R_6 can be $-\text{CH}_3$ or $-\text{CH}_2\text{CHOHCH}_3$. The product is an oligomer that exists as a mixture.

Foam preparation

PU were prepared using a one-pot and free-rise method. First, the components (2)–(5) and HMMM–PG were mixed by means of a high-speed stirrer (1800 rpm) for 1 min at room temperature until a uniform mixture was achieved. Then, component (6) was added to the reaction mixture, stirred again for an additional 10 s at the speed of 1800 rpm, and the mixture was quickly poured into an open paper mold ($250 \times 250 \times 60 \text{ mm}^3$) in order to obtain a free-rise foam. Finally, the PU materials were kept in an incubator at 60°C for 20 min to accelerate the curing process. After preparation, the samples were cut into the desired shapes and sizes according to the corresponding standards used for the evaluation of the different properties.

The formulations are listed in Table 1. The hydroxyl number for the HMMM–PG polyol is 447 mg KOH/g. For the three different samples, the total number of moles of $-\text{OH}$ in the polyether polyol is equivalent.

Measurements and characterization

Fourier transform infrared spectroscopy (FTIR) analysis

FTIR spectroscopy was performed using a ThermoFisher 6700 spectrometer at a resolution of 4 cm^{-1} with a total of 32 scans.

LC–MS analysis

Chromatographic analysis was performed with an Agilent 1260 Infinity apparatus: An Agilent G1312B SL binary pump and Agilent G1329B autosampler connected to a Agilent G1314B VWD detector (Agilent, California, USA). Analytes were separated with a 150-mm ZORBAX RRHT SB-C18 column at a temperature of 20°C maintained using a Agilent G1316A column oven. Detection was carried out using a microTOF-Q II ESI-Qq-TOF mass spectrometer (Bruker, Germany) that was used to monitor the total ion chromatogram for the mass range from $m/z = 0$ to $m/z = 3000$.

Thermogravimetric analysis

Thermogravimetric analysis (TGA) was performed using a Netzsch 209 F1 thermal analyzer at a heating

rate of 10 °C/min under a nitrogen atmosphere. The temperature range was from room temperature to 800 °C.

Compressive strength

The compressive strength was tested according to GB/T 8813-2008 with sheet dimensions of $100 \times 100 \times 100 \text{ mm}^3$.

Fire behavior

The limiting oxygen index (LOI) was obtained according to the standard GB/T 2406.2-2009. An oxygen index instrument (Rheometric Scientific Ltd.) was used on barrels with dimensions of $10 \times 10 \times 80 \text{ mm}^3$. The gross heat of combustion (HoC) was measured in an oxygen bomb calorimeter (Model 6200, IsoPeribol Oxygen Bomb Calorimeter, Parr Instrument Co., Moline, Illinois) according to the standard procedure ISO 1716:2010.

Morphological characterization

Scanning electron microscopy (SEM) experiments were performed using a Hitachi S-4800 scanning electron microscope. The micromorphology of the residual char after combustion with a conductive gold layer was observed by low-temperature fracturing under high vacuum with a voltage of 15 kV.

X-ray photoelectron spectroscopy (XPS)

XPS data were obtained using a Perkin Elmer PHI 5300 ESCA system at 250 W (12.5 kV at 20 mA) under a vacuum as high as 10^{-6} Pa (10^{-8} Torr). The char residues were obtained from the LOI tests. Typical results from XPS were reproducible within $\pm 3\%$, and the reported results are the average of three measurements.

Results and discussion

Characterization of HMMM-PG

Figure 1 shows the FTIR spectra of HMMM and HMMM-PG. The new peak at 3352 cm^{-1} , which was attributed to the stretching vibration of $-\text{OH}$, was noted in the spectrum of HMMM-PG, implying that

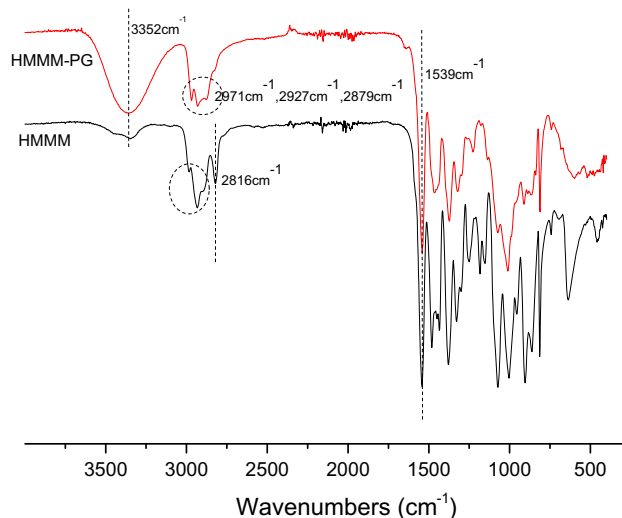


Figure 1 A comparison of the FTIR spectra of HMMM and HMMM-PG.

the reaction of HMMM with PG had occurred. The stretching vibration of $\text{C}=\text{N}$ in a triazine ring at 1539 cm^{-1} could be identified in the spectra of both HMMM and HMMM-PG. The peaks around $2879\text{--}2971 \text{ cm}^{-1}$ were associated with symmetric stretching vibrations of $-\text{CH}_3$ and $-\text{CH}_2$. The peak at 2816 cm^{-1} was assigned to the symmetric stretching vibration of $-\text{OCH}_3$. The deformation vibration of $-\text{CH}_2$ and anti-symmetric deformation vibration of $-\text{CH}_3$ were observed at 1460 cm^{-1} . In addition, the peak at 1376 cm^{-1} was due to the symmetric deformation vibration of $-\text{CH}_3$.

In order to study the composition of the HMMM-PG product, we applied HPLC separation coupled with MS detection using methanol as the mobile phase (Figs. 2, 3). The LC chromatograms of HMMM-PG showed five peaks at retention times of 9.4 min (peak 1), 11.6 min (peak 2), 15.5 min (peak 3), 17.5 min (peak 4), and 18.6 min (peak 5). In addition, Fig. 3 displays the mass spectrometry for the peaks at each retention time above with the peak numbers displayed in the parentheses of Fig. 3 referring to the peak numbers in Fig. 2, which confirmed that the five peaks in the LC chromatograms were attributed to five different ether exchanged products: HMMM-PG2, HMMM-PG3, HMMM-PG4, HMMM-PG5, and HMMM-PG6 whose chemical structure and molecular weight are illustrated in Table 2. Besides, HMMM-PG was detected using only MS (Fig. 4) to complement the results (Table 2). The relative intensity showed that the content in descending order of

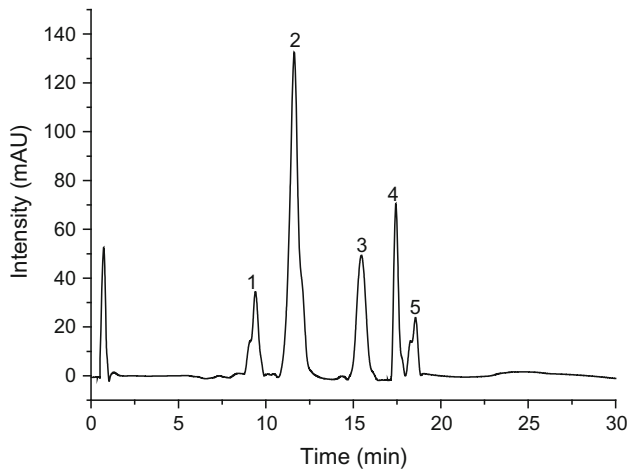


Figure 2 LC chromatograms of HMMM-PG by LC-MS.

the five different ether exchanged products was HMMM-PG6, HMMM-PG5, HMMM-PG3, HMMM-PG4, and HMMM-PG2.

Figure 5 shows the TG/DTG curves of HMMM-PG and 380A. 380A is a commercially available polyol. The temperature at 5% mass loss ($T_{0.05}$) was taken as the onset degradation temperature, which was observed at 181.1 °C for HMMM-PG and at 140.0 °C for 380A. The residue of HMMM-PG at 800 °C was 17.9%, while 380A decomposed completely at 382.8 °C without any residues. The apparent thermal stability of HMMM-PG higher than ordinary aliphatic polyols was most likely due to the stability of the triazine ring in the HMMM-PG structure [38].

The effect of shear rate on the shear viscosity of HMMM-PG at 25 °C is shown in Fig. 6. The shear viscosity of HMMM was in the range of 6.5–5.8 Pa s with a shear rate between 0 and 100 s^{-1} , while the shear viscosity values of HMMM-PG were within the range of 161–188 Pa s. HMMM-PG has higher shear viscosity than HMMM. The viscosity was dominated by the intermolecular hydrogen bonds of the nearby adjacent -OH groups [39]. However, at high shear rates (above 40 s^{-1}), the intermolecular hydrogen bonds are destroyed, leading to a sharp decrease in viscosity. This is helpful for foam processing.

Physical-mechanical properties and cell morphology of PU

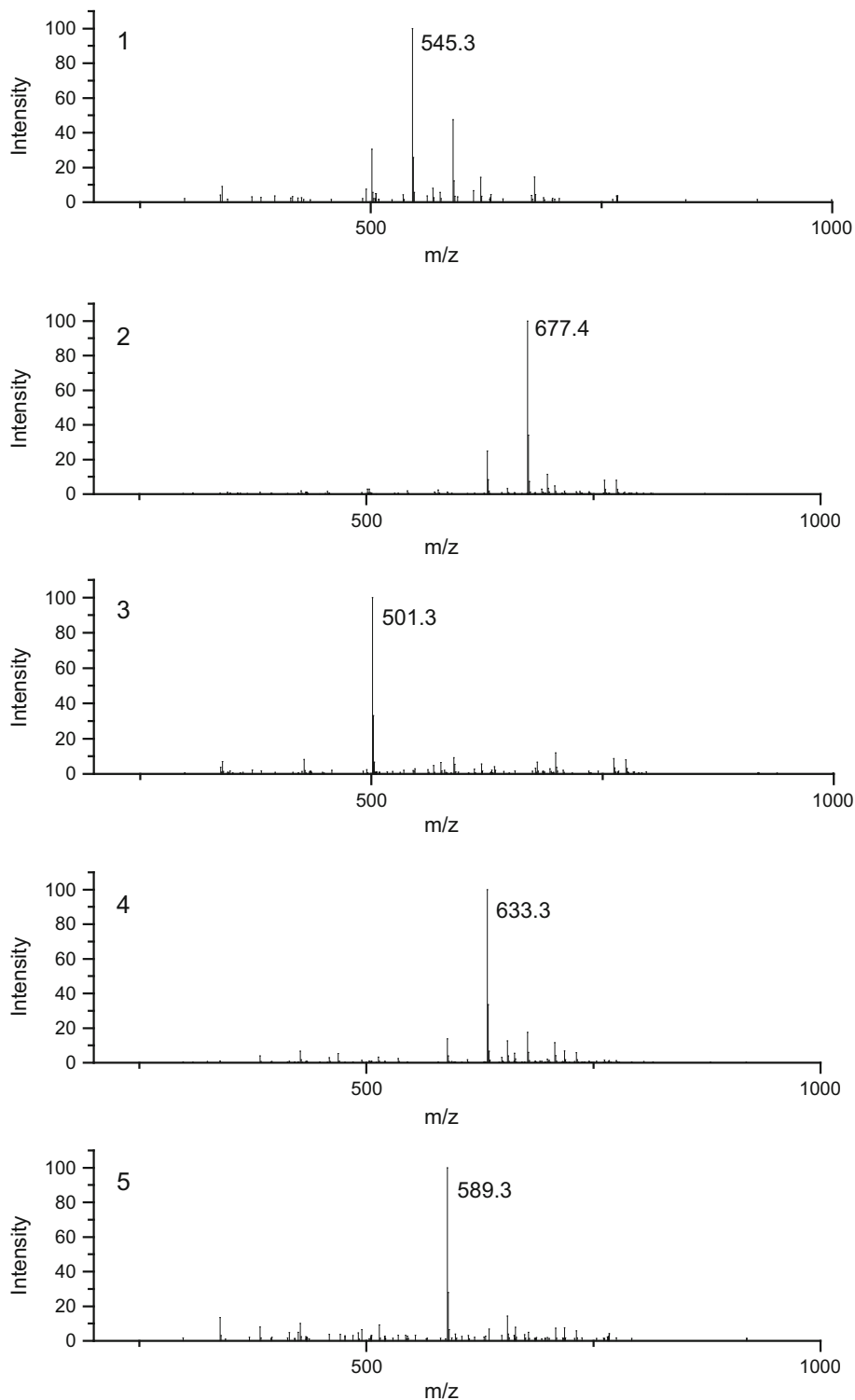
High compression strength and low thermal conductivity are desirable properties for polyurethane foams. Table 3 shows the compression strength,

thermal conductivity, and density of PUFs. The compression strength of the PUF:HMMM-PG sample was 0.15 MPa, which was three times higher than that found for the PUF with a commercial polyether polyol 380A (0.05 MPa). The compression strength of the PUF:380A/50%HMMM-PG sample (0.09 MPa) was between PUF:380A and PUF:HMMM-PG. This may be attributed to the higher degree of hydroxyl functionality, which increased the crosslinking density and the rigid triazine ring structures. In addition, the thermal conductivity of the PUF:HMMM-PG sample decreased when compared with the PUF:380A sample, which was due to the reduction of cell size (Fig. 7). In addition, the thermal conductivity of the PUF:380A/50%HMMM-PG sample (0.0267 W/m K) was between PUF:380A (0.0268 W/m K) and PUF: HMMM-PG (0.0260 W/m K). The density of PUF:380A, PUF:380A/50%HMMM-PG, and PUF: HMMM-PG were 36, 34, and 36 kg/m^3 , respectively. The difference in the density for each sample was small. The physical-mechanical properties of PUF depend on the rigidity of the polymer matrix, which on the other hand depends on the cell morphology of the foam. Figure 7 shows the SEM images of the prepared foams. The shapes of the cells in PUF:380A as well as in PUF:HMMM-PG are approximately spherical. The PUF:HMMM-PG sample shows a decrease in the average cell size with reference to PUF:380A.

The thermal behavior of PU

Figure 8 shows the TG and DTG curves obtained for PUF:380A, PUF:380A/50%HMMM-PG and PUF:HMMM-PG, and the data summarized in Table 4. The temperature at which a 5 wt% of weight loss takes place is defined as the initial degradation temperature (T_{onset}), and the temperature at which the degradation rate reaches a maximum is defined as T_{max} . The results show that the T_{onset} for PUF:380A was 140.6 °C and the T_{max} was 350.1 °C, which can be assigned to the degradation of the urethane linkages followed by the degradation of polyol and isocyanate [40]. Finally, the residue char of PUF:380A was 6.1 wt% at 800 °C under an N_2 atmosphere. For the PUF:HMMM-PG sample, the T_{onset} was 207.3 °C, while the T_{max} was 275.3 °C with a much weaker peak than that found for PUF:380A. The lower T_{max} can be attributed to the more unstable urethane groups formed by the reaction of HMMM-PG and

Figure 3 The mass spectra of HMMM-PG at a retention time of 9.4 min (peak 1), 11.6 min (peak 2), 15.5 min (peak 3), 17.5 min (peak 4), and 18.6 min (peak 5) from LC-MS.



isocyanate. In addition, the weaker thermal decomposition peak was attributed to the higher thermal stability of HMMM-PG. The peak in the range of 200–350 °C obtained for the PUF: HMMM-PG sample may be assigned to the thermal decomposition of

the urethane groups and the removal of PG in HMMM-PG, while the peak in the range 350–480 °C for the PUF: HMMM-PG sample was assigned to the thermal decomposition of polyol HMMM-PG and isocyanate. Besides, the residue at 800 °C for

Table 2 The assignment of each peak detected in LC–MS and MS

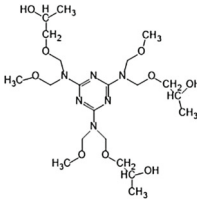
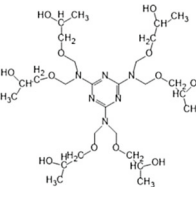
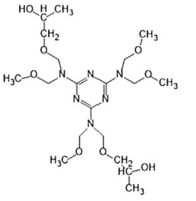
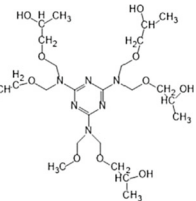
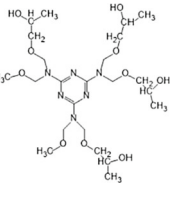
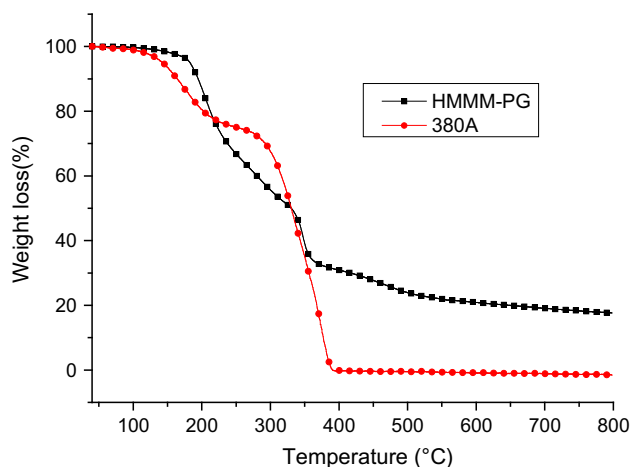
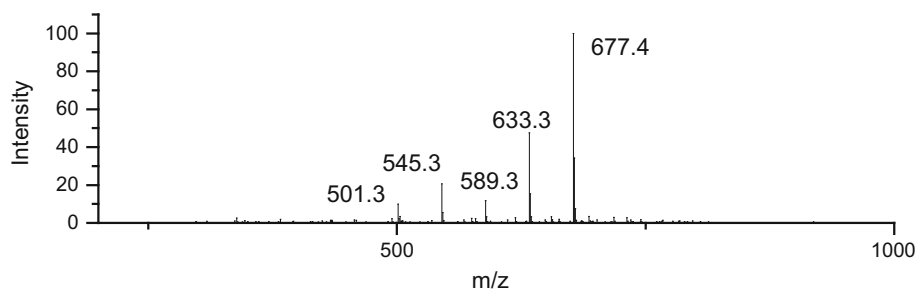
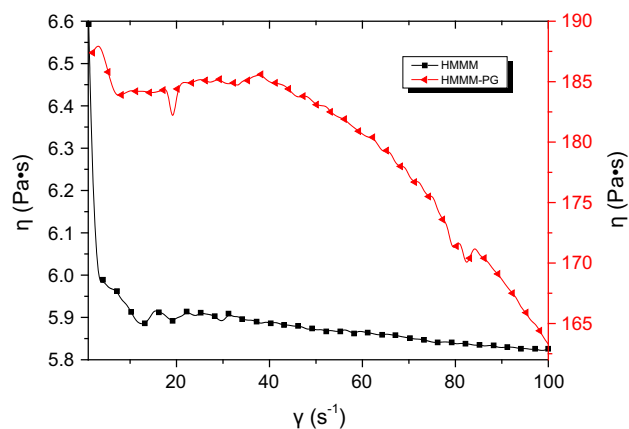
LC–MS (retention time min)	9.4	11.6	15.5	17.5	18.6
Chemical structure					
	(HMMM-PG3)	(HMMM-PG6)	(HMMM-PG2)	(HMMM-PG5)	(HMMM-PG4)
Molecular weight (g/mol)	522	654	478	601	566
MS m/z (relative intensity %)	545.3 [M-Na] ⁺ (20.6)	677.4 [M-Na] ⁺ (100)	501.3 [M-Na] ⁺ (9.8)	633.3 [M-Na] ⁺ (47.5)	589.3 [M-Na] ⁺ (11.7)

Figure 4 The mass spectra of HMMM–PG detected with MS.**Figure 5** TG curves of HMMM–PG and 380A.

PUF:HMMM–PG sample (19.1 wt%) was much higher than that observed for the PUF:380A sample (6.1 wt%). For the PUF:380A/50%HMMM–PG sample, there are two T_{max} which can be attributed to the thermal decomposition of polyols 380A-based polyurethane and polyols HMMM–PG-based polyurethane, respectively. In addition, the PUF:380A/

**Figure 6** Shear viscosity curves for HMMM and HMMM–PG.

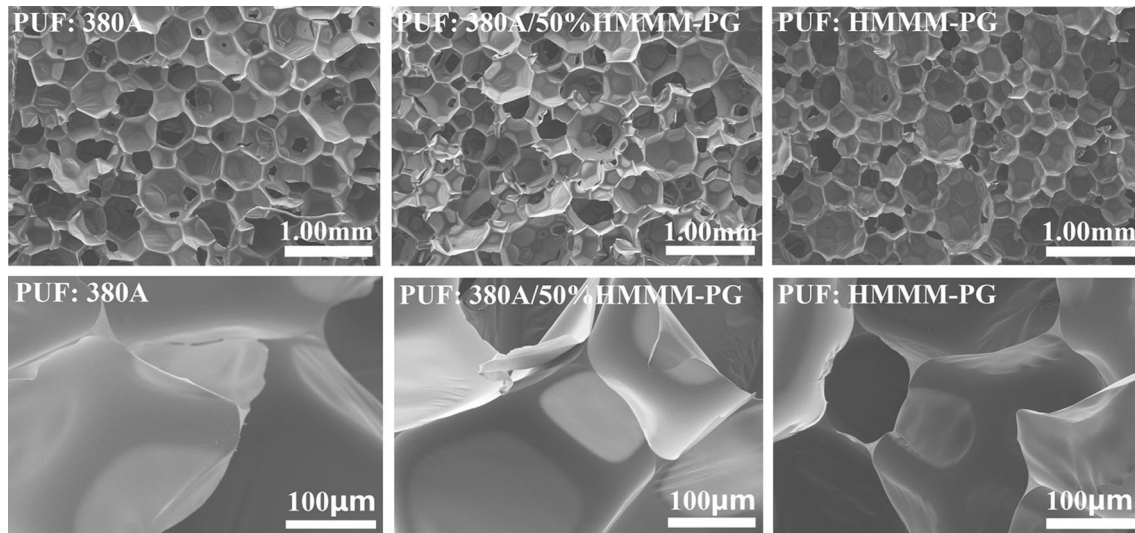
50%HMMM–PG sample's residue char was within the scope of PUF:380A and PUF: HMMM–PG.

The flame retardancy of PU

The LOI value obtained for PUF:380A was 18.8%, while the value for PUF:HMMM–PG was 20.9%. In addition, the LOI value obtained for PUF:380A/

Table 3 The mechanical properties of the prepared foams

Samples	PUF:380A	PUF:380A/50%HMMM-PG	PUF:HMMM-PG
Compression strength (MPa)	0.05	0.09	0.15
Thermal conductivity (W/m K)	0.0268	0.0267	0.0260
Density (Kg/m ³)	36	34	36

**Figure 7** SEM images of the prepared foams.

50%HMMM-PG was between the values of PUF:380A and PUF:HMMM-PG (19.6%) (Fig. 9). As a contrast, the LOI value of PUF using castor oil polyol was 19.9% [41]. The increased LOI value obtained using the polyether polyol HMMM-PG indicated the enhancing effect on flame retardancy. In detail, the combustion processes of the prepared foams at oxygen concentrations of 20.9% are illustrated in Fig. 10. Figure 11 also shows the digital photographs of combustion residues after the combustion test. For PUF:380A, the sample was ignited quickly with rapid flame propagation. Meanwhile, the char layer after combustion was too loose to keep its original shape, which can be seen in Fig. 11. Thus, the combustion residues curled with the spread of flame. For the PUF:380A/50%HMMM-PG sample, the sample was also ignited quickly with rapid flame propagation, while the combustion residues were strong enough to keep its original shape. However, for the PUF:HMMM-PG sample, during ignition, flame propagation apparently slowed down. Then, the flame gradually became smaller and finally extinguished within 15 s. In addition, the combustion residues also kept their original shape.

The HoC is the heat released by the complete combustion per unit mass of material, which can be used to evaluate the potential fire hazard of the construction materials [42]. The heat of combustion is determined by the elemental composition and the interactions between the components of a material. In general, the higher the content of C, the higher the HoC. Moreover, the higher the content of N, P, and O, the lower the HoC. Figure 9 shows the heat of combustion of each sample. The HoC for PUF:380A was 27.52 MJ/kg, but when substituted by HMMM-PG, it decreased to 26.97 MJ/kg. It could be seen that with the substitution of HMMM-PG, the HoC decreased gradually; the change in the LOI values shows an opposite trend. Therefore, the best fire performance was observed for the PUF:HMMM-PG foams.

Morphological characterization of the char residues

The morphologies of the char residues were characterized by SEM to further elucidate the flame-retardant performance of the char layer, and they are

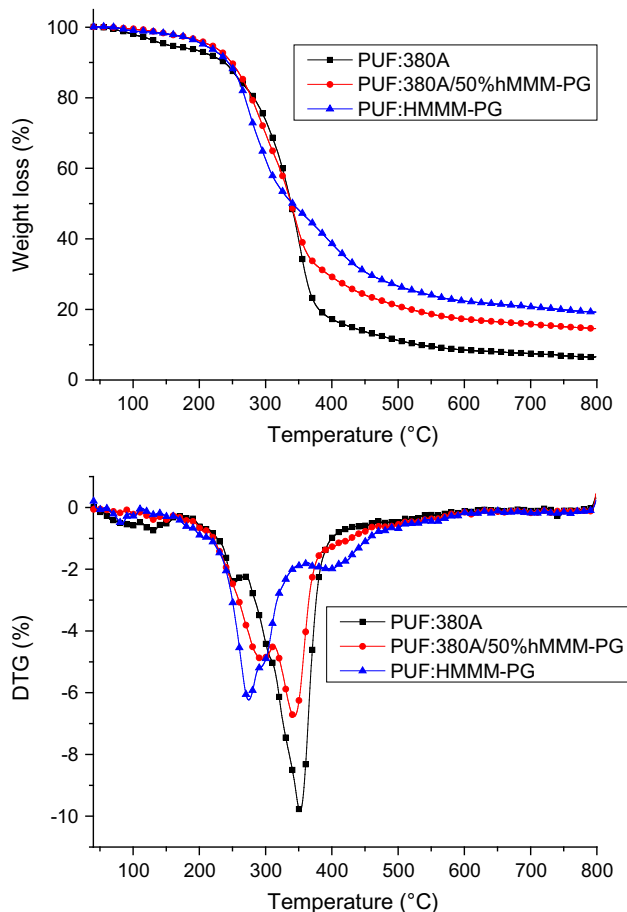


Figure 8 TG/DTG curves for PUF:380A, PUF:380A/50%hMMM-PG, and PUF:HMMM-PG.

displayed in Fig. 12. As seen in Fig. 12, the char residue of PUF:380A was porous with a lamellar morphology. During combustion, the flame and heat would pass through the gap and spread to the unburned portion. However, when using the polyether polyol HMMM-PG, the holes in the surface of carbon residue disappear and the surface of the carbon residues was continuous and dense. This continuous and dense char layer can hinder heat and

Table 4 TGA and DTG data for the various samples

Sample	T_{onset} (°C)	T_{max} (°C)	Residue at 800 °C (wt%)
PUF:380A	140.6	350.1	6.1
PUF:380A/50%hMMM-PG	207.3	291.4/341.7	14.4
PUF:HMMM-PG	207.3	275.3	19.1

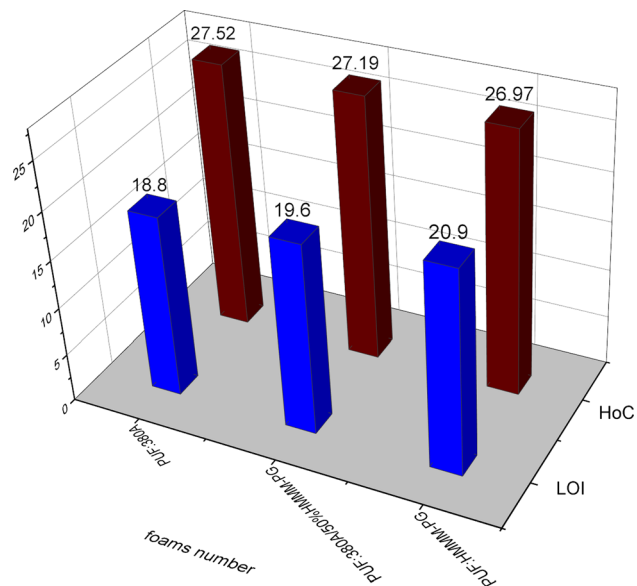


Figure 9 The heat of combustion and limiting oxygen index values obtained for each sample.

mass transfer between the gas and the condensed phases, and prevent the underlying polymeric substrate from further attack by heat flux [36].

XPS analysis of the char residues

The XPS data are listed in Table 5. In the combustion process, the N elements in the PU foams not only volatilize with the formation of gas such as NO_2 , but form relatively stable compounds containing C–N and C = N in the char residues [43]. The higher the relative content of N element in the char residue, the more stable the compounds containing N element after combustion and the higher the thermal stability of the material. It can be seen from Table 5 that the N/C ratio of PUF:HMMM-PG (0.048) was higher than that of PUF:380A (0.037), while the N/C ratio of PUF:380A/50%hMMM-PG (0.040) was between PUF:380A and PUF:HMMM-PG, which indicates

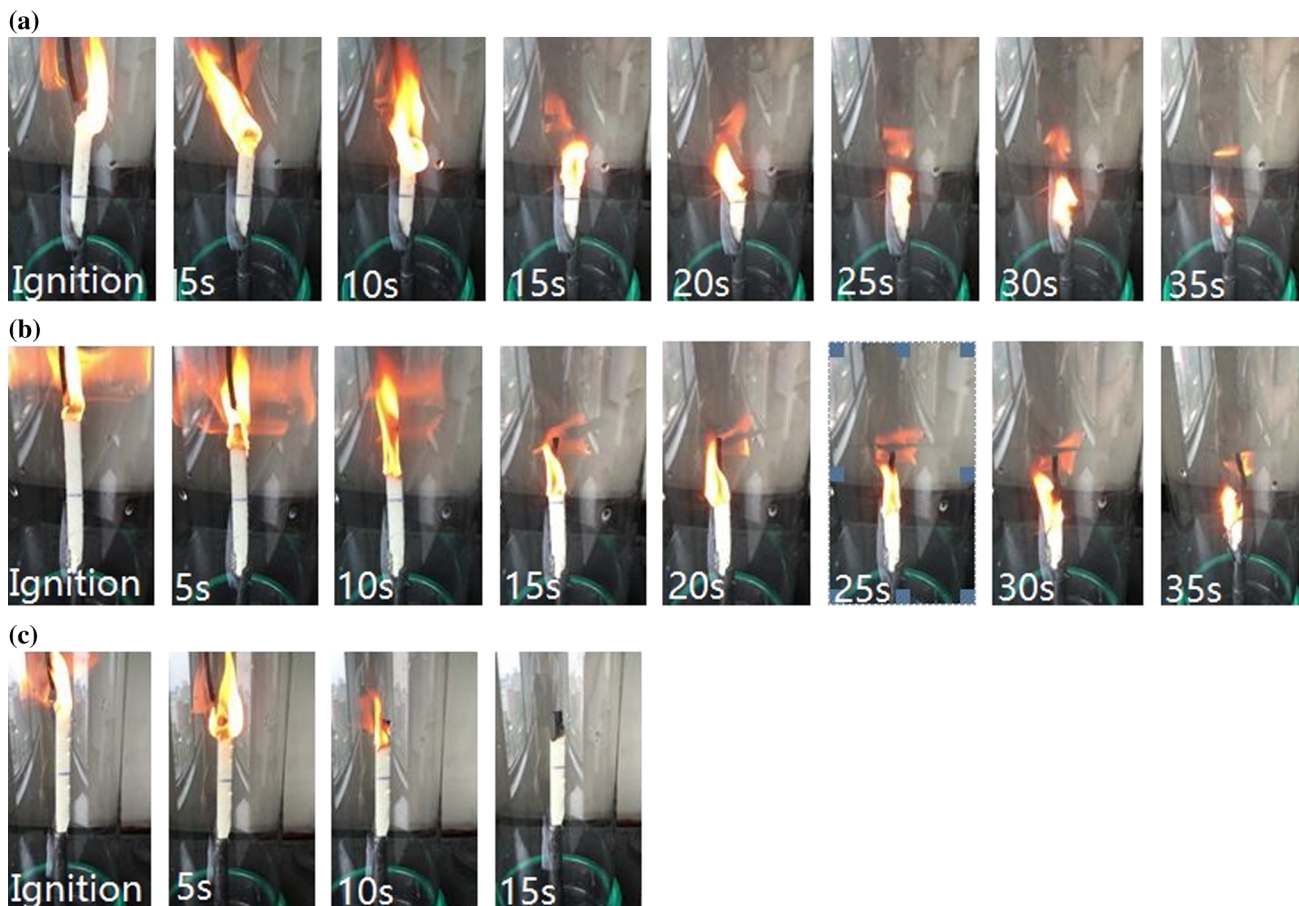


Figure 10 The combustion processes of the foams at oxygen concentrations of 20.9% (a PUF:380A, b PUF:380A/50%HMMM-PG, c PUF:HMMM-PG).



Figure 11 Digital photographs of the combustion residues after the combustion test.

that the use of polyether polyol HMMM-PG can improve the flame-retardant properties of PU foams. Further, the atomic percentage of oxygen in the char residues of PUF:380A/50%HMMM-PG and PUF:HMMM-PG was higher than that found for PUF:380A, which illustrates that foams using HMMM-PG have better char formation. The improvement in fire retardancy of PUF:HMMM-PG was mainly reflected in the condensed phase.

Conclusions

A new kind of melamine-based polyether polyol HMMM-PG was synthesized to prepare polyurethane foams. HMMM-PG began to decompose at 181.1 °C and had higher residues (17.9%) than the

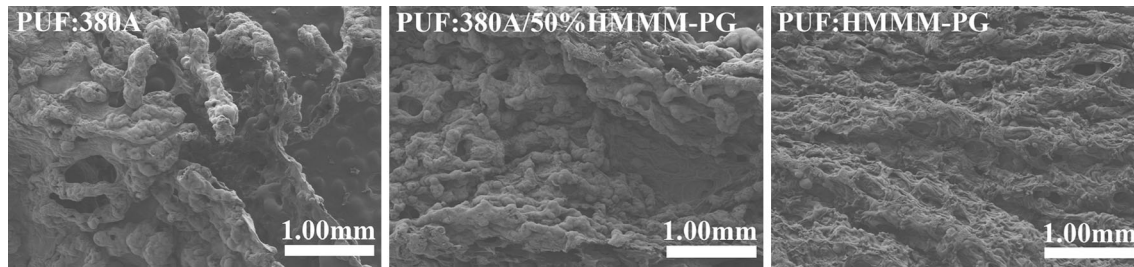


Figure 12 SEM micrographs of the char formed after combustion.

Table 5 XPS results obtained for the char residues

Sample	C (at.%)	N (at.%)	O (at.%)	N/C ratio
PUF:380A	79.24	2.95	17.81	0.037
PUF:380A/50%HMMM-PG	81.68	3.26	15.07	0.040
PUF:HMMM-PG	82.69	3.98	13.34	0.048

common polyol 380A. Besides, HMMM-PG displayed shear thinning because of the damage to the intermolecular hydrogen bonds with increasing shear rate. The compression strength of PUF:HMMM-PG (0.15 MPa) was 3 times higher than that found for PUF:380A (0.05 MPa), which was attributed to the higher degree of hydroxyl functionality that increased the crosslinking density and the rigid triazine ring structures. In addition, the thermal conductivity of the PUF:HMMM-PG sample decreased when compared with the PUF:380A sample. The flame-retardant properties of the foams could be significantly improved, which was mainly reflected in the condensed phase.

Funding The work was financially supported by the International Science & Technology Cooperation Program of China (No. S2014ZR0465).

Compliance with ethical standards

Conflict of interest The authors declare that they have no conflict of interest.

References

- [1] Oertel G (1993) Polyurethane Handbook, 2nd edn. Carl Hanser Publishers, Munich
- [2] Tang Z, Maroto-Valer MM, Andresen JM, Miller JW, Listemann ML, McDaniel PL (2002) Thermal degradation behavior of rigid polyurethane foams prepared with different fire retardant concentrations and blowing agents. *Polymer* 43:6471–6479
- [3] Hatakeyama H, Matsumura H, Hatakeyama T (2013) Glass transition and thermal degradation of rigid polyurethane foams derived from castor oil-molasses polyols. *J Therm Anal Calorim* 111:1545–1552
- [4] Engels HW, Pirkel HG, Albers RR, Albach W, Krause J, Hoffmann A, Casselmann H, Dormish J (2013) Polyurethanes: versatile materials and sustainable problem solvers for today's challenges. *Angew Chem Int Ed* 52:9422–9441
- [5] Bourbigot S, Duquesne SJ (2007) Fire retardant polymers: recent developments and opportunities. *Mater Chem* 17:2283–2300
- [6] Kim YS, Li YC, Pitts WM, Werrel M, Davis RD (2014) Rapid Growing Clay Coatings to Reduce the Fire Threat of Furniture. *ACS Appl Mater Interfaces* 6:2146–2152
- [7] Kaur R, Kumar M (2013) Function of silicon oil in the castor oil based rigid polyurethane foams. *J Polym Eng* 33:875–880
- [8] Usta N (2012) Investigation of fire behavior of rigid polyurethane foams containing fly ash and intumescent flame retardant by using a cone calorimeter. *J Appl Polym Sci* 124:3372–3382
- [9] Wilkie CA, Morgan AB (2009) Fire retardancy of polymeric materials, 2nd edn. CRC Press, Boca Raton
- [10] Levchik SV, Weil ED (2006) A review of recent progress in phosphorus-based flame retardants. *J Fire Sci* 24:345–362
- [11] Singh H, Jain AK (2009) Ignition, combustion, toxicity, and fire retardancy of polyurethane foams: a comprehensive review. *J Appl Polym Sci* 111:1115–1143
- [12] Modesti M, Lorenzetti A (2003) Improvement on fire behaviour of water blown PIR-PUR foams: use of a halogen-free flame retardant. *Eur Polym J* 39:263–268

- [13] Zhang P, Song L, Lu HD, Wang JA, Hu YA (2010) The thermal property and flame retardant mechanism of intumescent flame retardant paraffin system with metal. *Ind Eng Chem Res* 49:6003–6009
- [14] Yuan CY, Chen SY, Tsai CH, Chiu YS, Chen-Yang YW (2005) Thermally stable and flame-retardant aromatic phosphate and cyclotriphosphazene-containing polyurethanes: synthesis and properties. *Polym Adv Technol* 16:393–399
- [15] Liu YL, He JY, Yang RJ (2015) Effects of dimethyl methylphosphonate, aluminum hydroxide, ammonium polyphosphate, and expandable graphite on the flame retardancy and thermal properties of polyisocyanurate–polyurethane foams. *Ind Eng Chem Res* 54:5876–5884
- [16] Liu YL, He JY, Yang RJ (2015) The effects of aluminum hydroxide and ammonium polyphosphate on the flame retardancy and mechanical property of polyisocyanurate–polyurethane foams. *J Fire Sci* 33:459–472
- [17] Hale RC, Kim SL, Harvey E, La Guardia MJ, Mainor TM, Bush EO, Jacobs EM (2008) Antarctic research bases: local sources of polybrominated diphenyl ether (PBDE) flame retardants. *Environ Sci Technol* 42:1452–1457
- [18] Hale RC, La Guardia MJ, Harvey EP, Gaylor MO, Mainor TM, Duff WH (2001) Flame retardants—Persistent pollutants in land-applied sludges. *Nature* 412:140–141
- [19] Blum A (2007) The fire retardant dilemma. *Science* 318:194–195
- [20] König A, Fehrenbacher U, Kroke E, Hirth T (2009) Thermal decomposition behavior of the flame retardant melamine in slabstock flexible polyurethane foams. *J Fire Sci* 27:187–211
- [21] Awad WH, Wilkie CA (2011) Further study on the flammability of polyurea: the effect of intumescent coating and additive flame retardants. *Polym Adv Technol* 22:1297–1304
- [22] Wu K, Zhang Y, Hu W, Lian J, Hu Y (2013) Influence of ammonium polyphosphate microencapsulation on flame retardancy, thermal degradation and crystal structure of polypropylene composite. *Compos Sci Technol* 81:17–23
- [23] Levchik SV, Balabanovick AI, Levchik GF, Costa L (1997) Effect of melamine and its salts on combustion and thermal decomposition of polyamide 6. *Fire Mater* 21:75–83
- [24] Gijsman P, Steenbakkens R, Furst C, Kersjes J (2002) Differences in the flame retardant mechanism of melamine cyanurate in polyamide 6 and polyamide 66. *Polym Degrad Stab* 78:219–224
- [25] Weil ED, Levchik S (2004) Current Practice and Recent Commercial Developments in Flame Retardancy of Polyamides. *J Fire Sci* 22:251–264
- [26] Casu A, Camino G, Giorgi MD, Flath D, Morone V, Zenoni R (1997) Fire-retardant mechanistic aspects of melamine cyanurate in polyamide copolymer. *Polym Degrad Stab* 58:297–302
- [27] Braun U, Scharrel B, Fichera MA, Jager C (2007) Flame retardancy mechanisms of aluminium phosphinate in combination with melamine polyphosphate and zinc borate in glass-fibre reinforced polyamide 6,6. *Polym Degrad Stab* 92:1528–1545
- [28] Chen YH, Wang Q, Yan W, Tang HM (2006) Preparation of flame retardant polyamide 6 composite with melamine cyanurate nanoparticles in situ formed in extrusion process. *Polym Degrad Stab* 91:2632–2643
- [29] Lv P, Wang Z, Hu K, Fan W (2005) Flammability and thermal degradation of flame retarded polypropylene composites containing melamine phosphate and pentaerythritol derivatives. *Polym Degrad Stab* 90:523–534
- [30] Liu MF, Liu Y, Wang Q (2007) Flame-Retarded Poly(propylene) with Melamine Phosphate and Pentaerythritol/Polyurethane Composite Charring Agent. *Macromol Mater Eng* 292:206–213
- [31] Nyambo C, Kandare E, Wilkie CA (2009) Thermal stability and flammability characteristics of ethylene vinyl acetate (EVA) composites blended with a phenyl phosphonate-intercalated layered double hydroxide (LDH), melamine polyphosphate and/or boric acid. *Polym Degrad Stab* 94:513–520
- [32] Chen WY, Wang YZ, Chang FC (2004) Thermal and Flame Retardation Properties of Melamine Phosphate-Modified Epoxy Resins. *J Polym Res* 11:109–117
- [33] Thirumal M, Khastgir D, Nando GB, Naik YP, Singha NK (2010) Halogen-free flame retardant PUF: effect of melamine compounds on mechanical, thermal and flame retardant properties. *Polym Degrad Stab* 95:1138–1145
- [34] Czuprynski B, Liszkowska J, Paciorek-Sadowska J (2014) Modification of the Rigid Polyurethane-Polyisocyanurate Foams. *J Chem*. doi:10.1155/2014/130823
- [35] Lubczak J, Lukasiewicz B (2012) Oligoeterole i pianki poliuretanowe z pierooceniem 1,3,5-triazynowym i atomami boru. *Polimery* 57:819–829
- [36] Zhu HB, Peng ZM, Chen YM, Li GY, Wang L, Tang Y, Pang R, Khan ZUH, Wan PY (2014) Preparation and characterization of flame retardant polyurethane foams containing phosphorus–nitrogen-functionalized lignin. *RSC Adv* 4:55271–55279
- [37] Zhang M, Zhang JW, Chen SG, Zhou YH (2014) Synthesis and fire properties of rigid polyurethane foams made from a polyol derived from melamine and cardanol. *Polym Degrad Stab* 110:27–34
- [38] Chattopadhyay DK, Webster DC (2009) Thermal stability and flame retardancy of polyurethanes. *Prog Polym Sci* 34:1068–1133

- [39] Wu WQ, Tian HF, Xiang AM (2012) Influence of Polyol Plasticizers on the Properties of Polyvinyl Alcohol Films Fabricated by Melt Processing. *J Polym Environ* 20:63–69
- [40] Athanasia AS, David AC, Celine C, Darren JM, Pratheep KA (2015) A systematic study substituting polyether polyol with palm kernel oil based polyester polyol in rigid polyurethane foam. *Ind Crops Prod* 66:16–26
- [41] Li QF, Feng YL, Wang JW, Yin N, Zhao YH, Kang MQ, Wang XW (2016) Preparation and properties of rigid polyurethane foam based on modified castor oil. *Plast Rubber Compos* 45:16–21
- [42] Zatorski W, Brzozowski ZK, Kolbrecki A (2008) New developments in chemical modification of fire-safe rigid polyurethane foams. *Polym Degrad Stab* 93:2071–2076
- [43] Xu WZ, Liu L, Wang SQ, Hu Y (2015) Synergistic effect of expandable graphite and aluminum hypophosphite on flame-retardant properties of rigid polyurethane foam. *J Appl Polym Sci* 132:42842